Plant Growth Regulation (2020) 92:205–217
https://doi.org/10.1007/s10725-020-00631-2

ORIGINAL PAPER

New insights into the evolution and expression dynamics of invertase gene family in *Solanum lycopersicum*

Huawei Wei[1,2] · Songlin Chai[1,3] · Lei Ru[4] · Luzhao Pan[3] · Yuan Cheng[1] · Meiying Ruan[1] · Qingjing Ye[1] · Rongqing Wang[1] · Zhuping Yao[1] · Guozhi Zhou[1] · Yougen Chen[2] · Hongjian Wan[1,5]

Received: 7 December 2019 / Accepted: 23 May 2020 / Published online: 31 May 2020

Abstract

Invertases catalyze the irreversible hydrolysis of sucrose into glucose and fructose and thus play key roles in carbon metabolism and plant development. To gain insights into their evolutional and functional relationships, we conducted genome-wide analyses of invertase genes in tomato and other species, focusing on their evolution and expression dynamics. The analyses unexpectedly identified in the tomato genome 5 pseudo invertsase sequences and 5 non-functional cell wall invertases (CWINs) lacking the critical β-fructosidase motif or other amino acids required for hydrolyzing sucrose. Based on their phylogeny relationship and exon–intron structure, we speculated that the invertase gene family could arose from different ancestral genes. The acid invertase gene family, comprised of CWIN and vacuolar invertase (VIN), expanded through segmental and tandem duplication. Analysis of functional divergence suggests site-specific shifted evolutionary rate (Type-I) have played an important role in evolutionary novelties after acid invertase gene duplication in plants. Finally, paralogs within each of the CWIN, VIN and CIN subfamilies exhibited diverse expression responses to the same set of stress treatments including salt and temperature stresses, probably reflecting functional adaptability of the invertase genes during evolution.

Keywords Evolutionary patterns · Expression · Functional divergence · Gene duplication · Invertases · Tomato

Introduction

Sucrose (Suc), as the main end product of photosynthesis in most plants, is transported from the source leaves to sink tissues. In the heterotrophic sink organs, Suc is either irreversibly hydrolyzed by invertase (EC 3.2.1.26) into glucose (Glc) and fructose (Fru), or reversibly catalyzed by sucrose synthase (EC 2.4.1.13) into UDP-Glc and Fru (Braun et al. 2014). According to their optimum pH, invertases have been classified into two main types: neutral/alkaline invertases with an optimal pH of 7.0 to 7.8 and acid invertases with an optimum pH of 4.5 to 5.5 (Ruan et al. 2010). Among of them, acid invertases either tightly bound to cell wall (CWIN) or as a soluble form residing in the vacuole, hence, named as VIN. In contrast, neutral/alkaline invertases usually are located on cytoplasm, hence also called cytoplasmic invertase (CIN).

A growing number of evidences showed that CWINs play a key role in development and yield formation of plant, especially in sink organs where phloem unloading or subsequent postphloem transport follows an apoplasmic pathway (Ruan 2014). For example, mutation of *ZmCWIN2*, a CWIN

Huawei Wei and Songlin Chai have contributed equally to this work.

Electronic supplementary material The online version of this article (https://doi.org/10.1007/s10725-020-00631-2) contains supplementary material, which is available to authorized users.

✉ Hongjian Wan
wanhongjian@sina.com

1 State Key Laboratory for Managing Biotic and Chemical Threats to the Quality and Safety of Agro-Products, Institute of Vegetables, Zhejiang Academy of Agricultural Sciences, Hangzhou 310021, China

2 College of Horticulture, Anhui Agricultural University, Hefei 230036, China

3 College of Horticulture and Gardening, Yangtze University, Jingzhou 434025, China

4 Key Laboratory for Quality Improvement of Agricultural Products of Zhejiang Province, College of Agriculture and Food Science, Zhejiang A & F University, Lin'an 311300, Zhejiang, China

5 China-Australia Research Centre for Crop Improvement, Zhejiang Academy of Agricultural Sciences, Hangzhou 310021, China

expressed in the basal endosperm transfer cells of maize, led to miniature seed phenotype (Cheng et al. 1996). Similarly, transgenic suppression of its ortholog in rice, *GIF1* (renamed as OsCWIN2 by Ruan (2014)), reduced grain size (Wang et al. 2008). On the other hand, VINs appear to be largely involved in cell expansion through osmotic dependent or independent pathways (Wang et al. 2010) but could also play a role in cell division based on metabolite flux modelling (Beauvoit et al. 2014) and in modulating cell patterning through impacting on expression of MYB transcription factors and auxin signaling genes via VIN-mediated sugar signaling (Wang et al. 2014).

By contrast, much less is known about the function of CIN, a nonglycosylated enzyme. This may be attributable to the instability and low activity of CIN, compared with its highly glycosylated counterparts, CWIN and VIN (Ruan et al. 2010). CINs appear to exist in large numbers which can be further divided into α and β groups with the former targeting to mitochondria or plastids (Murayama and Handa 2007) and the latter functions in cytosol or nuclei (Barratt et al. 2009; Lou et al. 2007). Emerging evidence indicates that CINs are required for root and reproductive development (Lou et al. 2007; Welham et al. 2009) and may be involved in maintaining homeostasis of reactive oxygen species (Xiang et al. 2011).

In addition, plant invertase genes also play vital rules in plant response to abiotic stresses. In 2002, the researchers reported that soluble invertase is an early target of drought stress during the critical, abortion-sensitive phase of young ovary development in maize (Mathias et al. 2002). In 2012, the researchers also reported that high invertase activity in tomato reproductive organs correlates with enhanced sucrose import into, and heat tolerance of, young fruit (Li et al. 2012). Subsequently, Liu et al. found that cell wall invertase promotes fruit set under heat stress by suppressing ROS-independent cell death (Liu et al. 2016). Recently, *CsINV5*, a tea vacuolar invertase gene, can enhances cold tolerance in transgenic Arabidopsis (Qian et al. 2018). All these results showed that invertase genes could participate in plant response to abiotic stresses, including drought, heat and cold.

Recently, availability of plant whole genome sequencing will provide an opportunity to identify gene families (Lu et al. 2017; Chen et al. 2017; Sun et al. 2017; Guo et al. 2013; Gao et al. 2018; Zhang et al. 2017). In this study, a timely opportunity to examine invertase gene family has been provided by the sequencing of the tomato genome, with publicly available sequences from *S. lycopersicum* and its closest wild relative, *S. pimpinellifolium* (https://solgenomics.net/) and the availability of tomato expression profiles (https://ted.bti.cornell.edu/). Here, we conducted a comprehensive study on the evolution of invertase genes in tomato. The work uncovered several novel findings including (i) mass of pseudo or non-functional members were found in the acid invertase gene families in the tomato genome; (ii) segmental and tandem duplication account for acid invertase expansion; and (iii) paralogs from a given CIN, VIN or CWIN subfamilies of tomato exhibited diverse responses to stress treatment, indicating functional adaptability of the invertase genes during evolution.

Material and methods

Database searches and analyses

In this study, Hidden Markov Model (HMM) profile of Glyco_hydro_32N (PF00251), Glyco_hydro_32C domain (PF08244) and Glyco_hydro_100 domains (PF12899), which were typical N- and C-terminal conservation domains of acid invertase genes and conserved domain of CIN, downloaded from PFam (https://pfam.sanger.ac.uk/) were employed to identify the putative invertase genes from the tomato genomes, including *S. lycopersicum*, *S. pimpinellifolium* and *S. pennellii*. The BlastP search was performed using the HMM profile in SGN databases, followed by removal of redundant sequences from the above two methods. Sequences with an E-value over 10^{-10} and query over 50% were chosen as the candidates (Lu et al. 2017). All corresponding DNA and protein sequences of tomato invertase genes were downloaded and analyzed using NCBI's conserved domain search to identify typical N- and C-terminal domains in their protein structures, which was further confirmed with the Pfam database (www.sanger.ac.uk/Software/Pfam/search.shtml).

Invertase gene classification, chromosome mapping and duplication

The invertase genes in *S. lycopersicum* were categorized into different groups/subgroups based on classification in *Arabidopsis* invertase gene family. Their locations on tomato chromosomes were determined according to their positions given in the ITAG Release 2.4 in SGN (https://solgenomics.net). The tandem duplications of invertase genes were identified based on described in rice (Yang et al. 2008). The tandemly duplicated genes were defined as an array of two or more invertase genes with alignment e values $\leq 1 \times 10^{-25}$ in the range of 100-kb distance. The segmental gene duplications of tomato invertase genes were identified according to the method reported previously by Schauser et al. (2005), who found that an effective way to detect segmental duplication event was to identify additional paralogous protein pairs in the neighborhood of each of the family members.

Sequence alignment and phylogenetic analysis

Amino acid sequences of all invertase genes in tomato were aligned using Clustal X version 1.8 (Thompson et al. 1997), followed by manual adjustment. The phylogenetic tree was constructed by the NJ method using MEGA 5.0 software (Tamura et al. 2011). Bootstrapping (1000 replicates) was used to evaluate the degree of support for a particular grouping pattern in the tree. Branch lengths were assigned by pairwise calculations of the genetic distances, and missing data were treated by pairwise deletions of the gaps. For ML analysis, we used the software PhyML (version 3.0) and MrBayes (version 3.2.1) for phylogenetic tree construct. The parameters of the former are as follows: the Whelan and Goldman amino acid substitution model, g-distribution, and 100 nonparametric bootstrap replicates (Guindon and Gascuel 2003). For latter: the fixed Whelan and Goldman model, four Markov chains, and an average SD of 0.01 (Ronquist and Huelsenbeck 2003). Model selection was performed using the ProtTest (version 2.4) software (Abascal et al. 2005).

Analysis of functional divergence

DIVERGE 3 software (Gu et al. 2013) was used to evaluate the potential functional divergence and to predict the important amino acid residues in these families. The coefficients of type I and II functional divergence (θ_I and θ_{II}) between CWIN and VIN families were estimated through posterior analysis. A θ_I or θ_{II} value significantly > 0 indicates altered selective constraints or a radical shift in amino acid physiochemical properties after gene duplication and/or speciation (Gu 1999, 2006). Moreover, based on the posterior probability (Q_k), a site-specific profile was also used to predict amino acid residues that were important for functional divergence.

Subcellular localization of tomato VIN and CIN fusion proteins

Two tomato invertases were experimentally assayed for their specific subcellular localization, namely, *SlVIN*2 (a vacuolar invertase, VIN) and *SlCIN*3 (a cytoplasmic invertase belonging to β clade, CIN). Their full-length cDNAs without stop codon were amplified using gene specific primers (Supplemental Table S1). The amplicons were inserted into the CaMV35S-EGFP-NOS sequence of a pCV-eGFP expression vector to generate cauliflower mosaic virus 35S promoter-driven GFP fusion constructs. A set of plant organelle RFP markers, which were localized in the tonoplast and mitochondria, respectively (Nelson et al. 2007), were used as co-localization markers in this experiment.

Transient expressions of the SlVIN2:eGFP and SlCIN3:eGFP along with their respective tonoplast or mitochondrial RFP markers were performed by particle bombardment in onion epidermis as previously described (Jin et al. 2009; Wang et al. 2010). A PDS-1000/He Biolistic particle-delivery system (Bio-Rad) was used by following the manufacturer's protocol. GFP- and RFP-expressing cells were detected with a Leica TCS SP5 confocal laser scanning microscope system (Leica Microsystems, Bannockburn, IL, USA) with argon laser excitation wavelengths of 488 nm (GFP) and 568 nm (RFP), respectively.

Differential gene expression profiles based on RNA-seq

To generate the expression profiles of invertase genes among different organs and development stages, the RNA-seq data from various tissues in cultivated tomato (*S. lycopersicum* var Heinz) and the wild relative (*S. pimpinellifolium*) were downloaded from the TOMATO FUNCTIONAL GENOMICS DATABASE (TFGD) (https://ted.bti.cornell.edu/). Normalized gene expression values were estimated by fragments per kilobase pair of exon model per million fragments mapped (FPKM). Finally, log2-transformed FPKM values of invertase genes in these tissues were used to draw heatmaps. To avoid taking the log of a number less than 1, all such FPKM values were replaced by 1. The expression data were hierarchically clustered based on MeV 4.5 software (Saeed et al. 2003).

Plant material for stress treatments

A tomato (*S. lycopersicum*) cultivar, zhefen702, was selected for stress treatments. Seeds were germinated in water-saturated filter paper in a petri dish. Geminated seedlings were grown on Hoagland nutrient solution in growth chambers (25 °C/18 °C day/night, 12 h/12 h light/dark cycle) (Paiva et al. 1998). The relative humidity was kept at 65% to 75%. Seedlings at the fourth true leaf stage were used for stress treatments. For salt and drought treatments, seedlings were transferred to Hoagland solution but containing 150 mM NaCl or 400 mM PEG (6000). For cold and heat shock treatments, the seedlings were kept in the artificial climate chamber at 4 ± 1 and 42 ± 1 °C, respectively. Leaves were collected at 0, 1.5, 3, 6, 12, and 24 h after each treatment. All these leaf samples were snap-frozen in liquid and stored at − 80 °C for RNA extraction. Three biological replications were assayed for each treatment.

RNA extraction and cDNA synthesis and qRT-PCR

Total RNA was isolated from each sample using TRIzol reagent (Invitrogen Ltd., Paisley, Renfrewshire, UK) according to the manufacturer's protocols and was treated with DNase I (Promega, Madison, WI, USA) to remove any traces of

genomic DNA. The first strand cDNA was synthesized using the RNA PCR Kit Version 2.1 (Takara, Tokyo, Japan).

Primers for qPCR were designed using Primer 5.0 (Premier Biosoft International, Palo Alto, CA) (Supplemental Table S1). qRT-PCR was performed in a 96-well plate with a StepOnePlus ™ Real-Time PCR System (Applied Biosystems, Foster City, CA, USA) using SYBR Green-based PCR assay. Each 20 µl reaction mixture contained 10 µl of 2 × SYBR Green PCR Master Mix reagent (Applied Biosystems), 1 µl of diluted cDNA, 0.4 µl (250 nmol) of each gene-specific primer and 8.2 µl of ddH_2O. PCR was run at the following condition: 95 °C for 10 min, 40 cycles of 95 °C for 30 s, 55 °C for 30 s, and 68 °C for 45 s. Three biological replicates were used for each treatment for all the invertase genes studied and each biological replication was carried out in triplicate. The reference gene, GAPDH (U97257), was used for normalization of the expression level of invertase genes in tomato (Expósito-Rodríguez et al. 2008). Quantification analysis was performed using the $2^{-\Delta\Delta Ct}$ method (Livak and Schmittgen 2001).

Results

Identification and sequence analysis of acid invertase gene families in the tomato genome

Through multiple bioinformatics analyses (see "Material and methods"), a total of 13 putative acid invertase gene sequences was identified (Supplemental Table S2). Among them, nine of which are predicted to target to the cell wall and four targeted to the vacuoles according to prediction analyses using PSORT (https://psort.hgc.jp/). We further found that there were two sequences, each of which missed significant portion(s) of the coding region, hence most likely encoding truncated protein (Supplemental Table S2). Therefore, these 2 members were excluded from the subsequent analysis. Table 1 shows the characteristics of the 11 putative CWINs and VINs, including sizes of their open reading frames (ORF), protein molecular weight and *pI* values.

The analysis revealed that the presence/absence of four amino acids (NDPN) known to be essential for recognition and stable binding of sucrose (Alberto et al. 2004; Lammens et al. 2009) in *SlCWIN* 1 to 4 and *SlCWIN* 5 to 8, respectively (Fig. 1). Since this motif 'NDPN' is indispensable for the transfructosylation capability (Schroeven et al. 2008), *SlCWIN 5* to *8* could not encode catalytically active acid invertases, rendering them incapable to hydrolyze sucrose, hence are non-functional (Le Roy et al. 2013). Furthermore, an amino acid substitution was found in *SldeCWIN*1 (A instead of D at 239), a characteristic of defective cell wall invertases (deCWINs) unable to hydrolyze sucrose (Le Roy et al. 2013). Thus, the analyses identified 5 non-functional or defective CWIN members. Interestingly, all the 4 functional and 5 defective CWINs contain the second motif WECXDF (Fig. 1), which is required for the catalytic activity of CWINs (Sturm and Chrispeels 1990).

Table 1 Key features of acid invertase genes in tomato

Gene name	SGN locus	Gene reported[a]	No. of exons[b]	ORF length[c] (bp)	Deduced polypeptide			Chromosome no
					Length[d] (aa)	Mol wt[e] (kDa)	p*I*[f]	
SldeCWIN1	Solyc03g121680		6	1716	571	64.18	6.80	3
SlCWIN1	Solyc09g010080	Lin5	6	1755	584	67.21	9.20	9
SlCWIN2	Solyc10g083290	Lin6	6	1749	582	65.87	9.23	10
SlCWIN3	Solyc09g010090	Lin7	6	1752	583	66.19	6.93	9
SlCWIN4	Solyc10g083300	Lin8	6	1770	589	66.88	8.94	10
SlCWIN5	Solyc06g064620		8	1683	560	63.09	5.14	6
SlCWIN6	Solyc10g085360		5	1728	575	65.56	8.79	10
SlCWIN7	Solyc10g085640		7	1674	587	63.75	6.95	10
SlCWIN8	Solyc10g085650		5	1728	575	66.30	6.52	10
SlVIN1	Solyc03g083910	TIV1	7	1947	582	71.36	5.54	3
SlVIN2	Solyc08g079080		7	1959	652	72.79	6.21	8

[a]These genes had been reported previously (Fridman and Zamir 2003; Fridman et al. 2004)

[b]No. of exons with coding domain sequence

[c]Length of open reading frame

[d]Length (no. of amino acid) of the deduced polypeptide

[e]Molecular weight of the deduced polypeptide in Dalton

[f]Isoelectric point of the deduced polypeptide

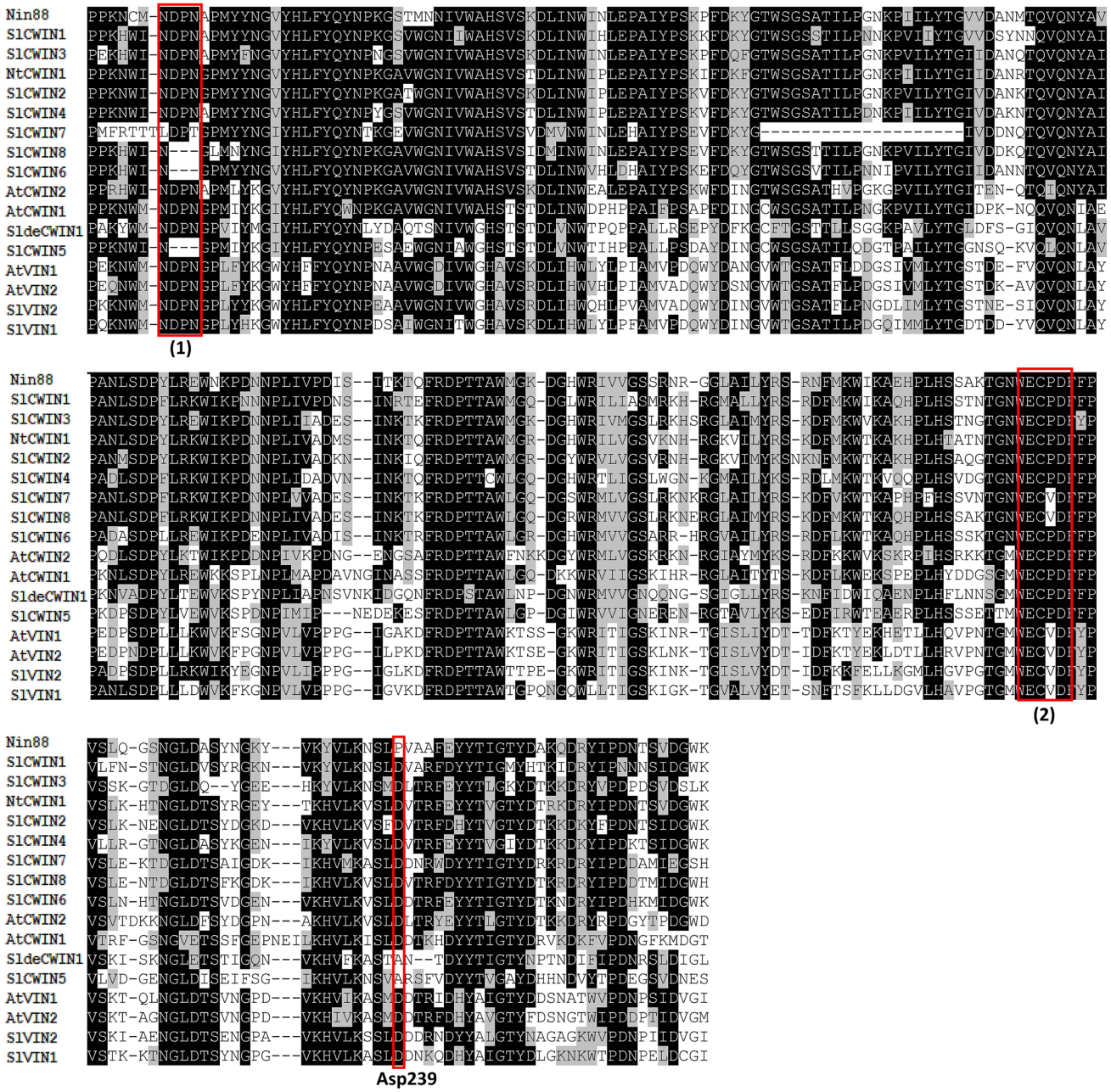

Fig. 1 Multiple sequence alignment of acid invertases. Two conserved domains and one critical amino acid (Asp239) were indicated in red box: 1 β-fructosidase motif (NDPN) and 2 cysteine catalytic domain (WECP/VD). There are five putative CWINs which contain both two conserved domains (SldeCWIN1, SlCWIN1, SlCWIN2, SlCWIN3, and SlCWIN4). However, the critical amino acid Asp239, required for hydrolyzing sucrose was mutated in SldeCWIN1, indicating it may not function as CWIN. For the other four putative CWINs (SlCWIN5, SlCWIN6, SlCWIN7, SlCWIN8), they all lost β-fructosidase motif. Accession numbers or Locus ID for all tomato invertases were listed in Supplemental Table S2. Those for other species are: Tobacco Nin88 (AF376773), NtCWIN1 (X81834), AtCWIN1 (At3g13790), AtCWIN2 (At3g52600), AtVIN1 (At1g62660), AtVIN2 (At1g12240), AtVIN1 (At1g62660), AtVIN2 (At1g12240). Species abbreviations: Nt: *Nicotiana tabacum*, At: *Arabidopsis thaliana*, Sl: *Solanum lycopersicum*

For VINs, apart from the previously characterized *TIV1* (named as *SlVIN1* here), we identified a second putative *VIN*, *SlVIN2* (Fig. 1). Their encoded proteins share high sequence homology with the Arabidopsis counterparts, *AtVIN1* and *AtVIN2* and featured with cysteine catalytic domain as WEC**V**D (Fig. 1), a hallmark of VIN, instead of WEC**P**D observed in CWINs (Ji et al. 2005). In addition, the members of neutral/alkaline invertase sub-family had been identified (Pan et al. 2019).The eight CINs fall into α and β subgroups that differed consistently in eight amino acids

(Boxed regions in Supplemental Fig. S1) reported in rice and *Arabidopsis* (Ji et al. 2005).

Subcellular localization of representative tomato VIN and CIN genes

In this paper, we selected one member from each of the two subgroups to experimentally verify their subcellular localizations using C-terminal green florescent protein (GFP) fusion constructs. A plant tonoplast or mitochondrial marker fused with RFP (Nelson et al. 2007) was co-bombarded with SlVIN2:eGFP and SlCIN3:eGFP, respectively, to help determine the subcellular locations of these invertases.The analyses revealed that in the plasmolyzed onion epidermal cells, the SlVIN2:eGFP fluorescence was distributed throughout the vacuole (Fig. 2a), whereas the RFP tonoplast marker signals were concentrated in the membrane region (Fig. 2b). After overlaying the two images, co-localization of SlVIN2:eGFP and tonoplast RFP marker was evident (arrowheads), with the former appearing also inside the vacuole where tonoplast marker (RFP) signals were absent (Fig. 2c, arrows), as expected. For SlCIN3, a tomato cytoplasmic invertase of the β clade, its eGFP fluorescence displayed evenly throughout the cytosol (Fig. 2d), whereas the mitochondrial marker (RFP) signals exhibited inside the cytosol in a dotted pattern (Fig. 2e, arrows). Overlaying the two images revealed localization of SlCIN3:eGFP signals in the cytosolic regions where the mitochondrial RFP markers was absent (Fig. 2f, arrows), indicating that *SlCIN3* is localized in the cytosol.

Genomic distribution and gene duplication

Chromosomal mapping revealed that the tomato acid invertase genes are located on five of the twelve chromosomes (Fig. 3) where they exhibited a high variation in their distributions. Here, a maximum number of five genes (*SlCWIN 2*, *4*, *6*, *7* and *8*) were mapped on chromosomal 10 closely followed by two genes on each of chromosome 3 and 9. On the contrary, each of chromosomes 6 and 8 contained only one gene (*SlCWIN5* and *SlVIN2*, respectively).

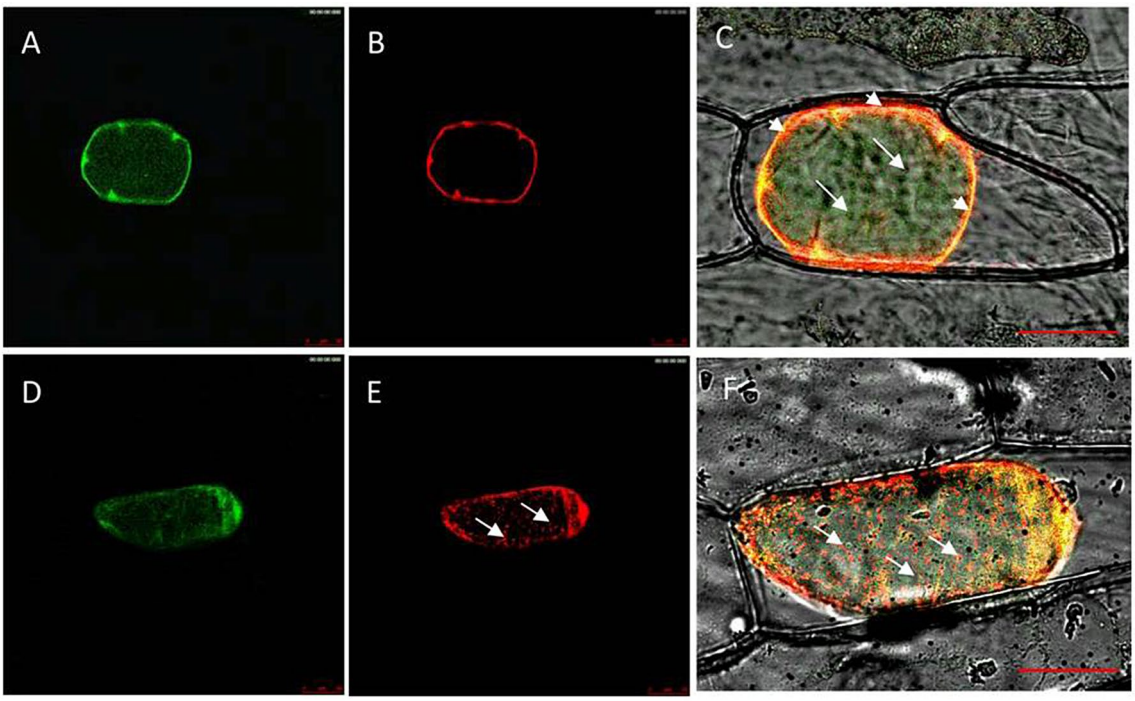

Fig. 2 Subcellular localization of seleted invertases in tomato, **a** to **c** subcellular co-localization of SlVIN2:eGFP, and the plant tonoplast organelle marker (RFP) fusion proteins in plasmolyzed onion epidermal cells after co-bombardment. Note that the SlVIN2:eGFP signals were distributed throughout the vacuole (**a**), whereas the tonoplast marker (RFP) signals were concentrated in the tonoplast and regions nearby (**b**). After overlaying the two images (**c**), co-localization of SlVIN2:eGFP and tonoplast marker (RFP) was evident (arrowheads), with the former appearing also inside the vacuole (arrows) where tonoplast marker (RFP) signals were absent. **d** to **f** subcellular co-localization of SlCIN3:eGFP, and the plant mitochondrial organelle marker (RFP) fusion proteins in plasmolyzed onion epidermal cells after co-bombardment. Note that the SlCIN3:eGFP signals were evenly distributed throughout the cytosol (**d**), whereas the mitochondrial marker (RFP) signals were distributed inside the cytosol as dots (**e**, arrows). After overlaying the two images (**f**), localization of SlCIN3:eGFP signals in the cytosol was observed, where the mitochondrial RFP marker signal was absent (arrows indicating the SlCIN3:eGFP signals not overlaid by the RFP signals). Bars = 50 µm

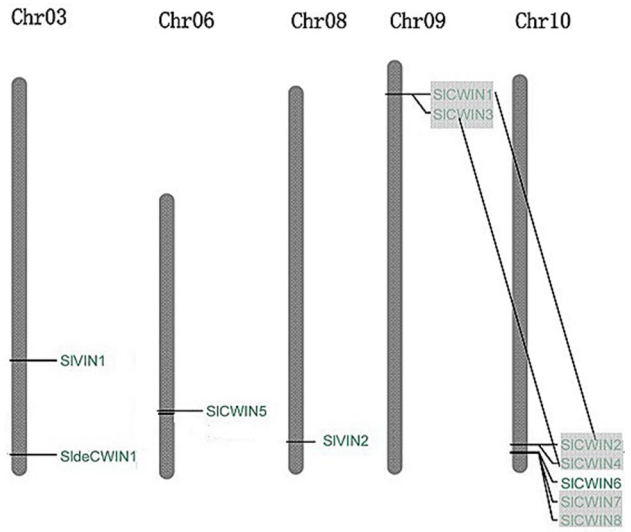

Fig. 3 Chromosome numbers are indicated at the top of the chromosomes. The acid invertase genes were in green font, respectively. The lines connecting the invertase genes represent segment duplicated genes, whereas the tandem duplicated gene clusters are highlighted in grey shaded boxes

Segmental duplication and tandem duplication played an important role in gene family expansion during evolution (Cannon et al. 2004). Here, evidence of segmental genome duplications was identified for the *SlCWIN1* and *SlCWIN3* chromosomal regions (Fig. 3), which show synteny with the surrounding genomic regions containing *SlCWIN2* (chromosome 10), and *SlCWIN4* (chromosome 10), respectively. Three pairs of genes (*SlCWIN*1/*SlCWIN*3, *SlCWIN*2/*SlCWIN*4 and *SlCWIN*7/*SlCWIN*8) were found to be tandem-duplicated (Supplemental Table S3, Fig. 3) and were placed juxtaposed with no intervening gene. Of them, the former two pairs of CWINs were identified previously to be tandemly duplicated (Fridman and Zamir 2003). The distance between these invertase genes ranged from 2.911 to 9.612 kb (Supplemental Table S3). The overall similarity of the coding sequences of these genes ranged from 75.53% to 81.72% (Supplemental Table S3, Fig. 3). In summary, tandem duplication and segmental duplication events were observed in *CWINs* (Fig. 3). However, for neutral/alkaline invertases, no duplication event was observed in their duplication (Pan et al. 2019).

Functional divergence among acid invertase genes

We further investigated whether amino acid substitutions in acid invertase gene family could have caused adaptive functional diversification in tomato and potato.Comparison of these two groups of acid invertase proteins was performed, and the rate of amino acid evolution in each sequence position was estimated. The analysis revealed that the coefficient of type-I functional divergence (θ_I) between CWINs and VINs groups was significantly greater than 0 ($\theta_I = 0.437 \pm 0.06$, $P < 0.05$). This observation suggests that the site-specific altered functional constraint on the CWIN and VIN groups is statistically significant and that some amino acid sites may be subjected to different site-specific shifts in evolutionary rate that can lead to a subgroup-specific functional evolution after their divergence from an ancient common ancestor. However, in contrast to the findings on type-I functional divergence, no statistical evidence for type-II functional divergence (θ_{II}) was observed between CWINs and VINs groups ($\theta_{II} = 0.06 \pm 0.08$, $P > 0.05$). This finding suggests that type-I functional divergence may have played an important role in evolutionary novelties after acid invertase gene duplication in plants.

The critical amino acid residues responsible for the functional divergence were further identified by analyzing the site-specific profile in combination with a posterior probability (Q*k*). Among all of the aligned sites, the Q*k* values of most sites were smaller than 0.75 (Fig. 4a). Therefore, in order to reduce false positive, $Qk > 0.75$ was selected as a cut-off value to identify critical amino acid residues related to type-I functional divergence between CWIN and VIN groups. Thirty-three amino acid residues were predicted to be type-I functional divergence related ($Qk > 0.75$) (Supplemental Fig. S2). Sequence alignment revealed high conservation of these amino acid residues among CWIN and VIN subgroups (Fig. 4b). Of them, site 453 was predicted to be most highly related to functional divergence since it has the highest Q*k* value of 0.94. On the contrary, the lowest degree of relation was observed at site 621 with a Q*k* value of 0.75 (Fig. 4c).

Wild and cultivated tomato species share similar expression patterns of invertase genes but with divergence in the expression of some defective invertase genes

Global expression differences and tissue-specific expression patterns of genes were helpful to understand their function in plant species (Guo et al. 2018; Pang et al. 2017; Zhao et al. 2013; Lü et al. 2013). In this study, we found that all the eight CINs are highly expressed in the ovary, seed and fruit tissues (Fig. 5a). The near constitutive expression patterns of CINs were equally observed in 5–10 days developing fruit and seed except for *SlCIN 6* and *8* (Fig. 5b). The CWINs also showed similar expression patterns between the two species. Here, *SlCWIN1* (*LIN5*) was highly expressed in flower and young fruit of both wild (Fig. 5a) and cultivated species (Fig. 5b) while *SlCWIN3* (*LIN7*) was mainly expressed in flower and seed tissues with no or little expression in fruit tissues (Fig. 5a and b). In contrast to *SlCWIN1* and *3* that

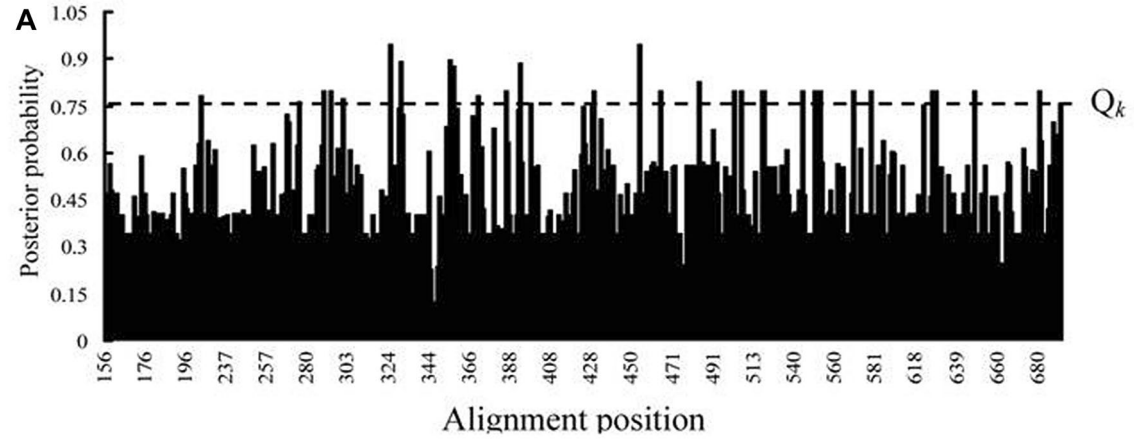

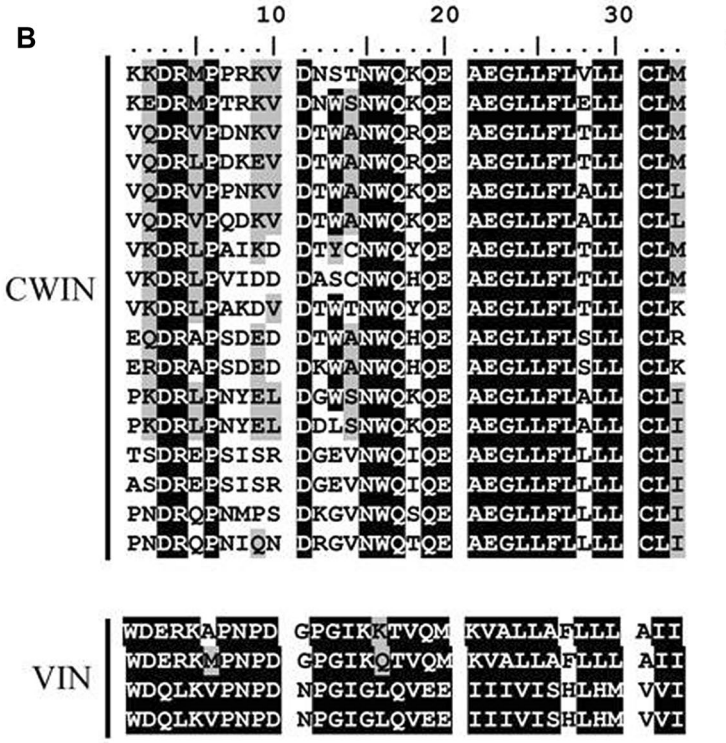

C

Site	Q_k	Site	Q_k
203	0.78	483	0.82
275	0.76	500	0.80
287	0.80	504	0.80
292	0.80	517	0.80
298	0.77	518	0.80
324	0.94	543	0.80
329	0.89	549	0.80
355	0.90	552	0.80
357	0.87	568	0.80
369	0.78	578	0.80
385	0.80	621	0.75
392	0.89	626	0.80
397	0.76	628	0.80
427	0.76	647	0.80
428	0.80	680	0.80
453	0.94	690	0.76
464	0.80		

Fig. 4 A site-specific profile based on the posterior probability (Qk) was used to identify the critical amino acid sites responsible for the functional divergence between CWIN and VIN subfamilies. According to the definition, a large Qk value indicates a high possibility that the functional constraint of a site is different between the two subfamilies. **a** Site-specific profile for predicting critical amino acid residues responsible for the gene specific type I functional divergence between CWIN and VIN subfamilies, measured by posterior probability. **b** CWIN and VIN subfamilies and **c** Qk values of 33 amino acid sites

did not express in roots and leaves, *SlCWIN 2* and *4* (*LIN6* and *8*) were mainly expressed in vegetative tissues in both species (Fig. 5). These findings are consistent with previous reports (Fridman and Zamir 2003; Godt and Roitsch 1997). Interestingly, the five defective or non-functional CWIN genes (*SlCWIN5-8* and *SldeCWIN1*) were generally weakly expressed in both species, except for *SlCWIN5* and *SlCWIN6* expressed in developing seed of the wild species (Fig. 5a). By contrast, neither *SlCWIN5* nor *SlCWIN6* displayed high expression in the seed or fruit tissues of the cultivated species (Fig. 5b). For the two VIN genes, *SlVIN1* (*TIV1*) were constitutively expressed in all the tissues examined while *SlVIN2* (*LIN9*) was mainly expressed roots, flower and fruit tissues across both species (Fig. 5).

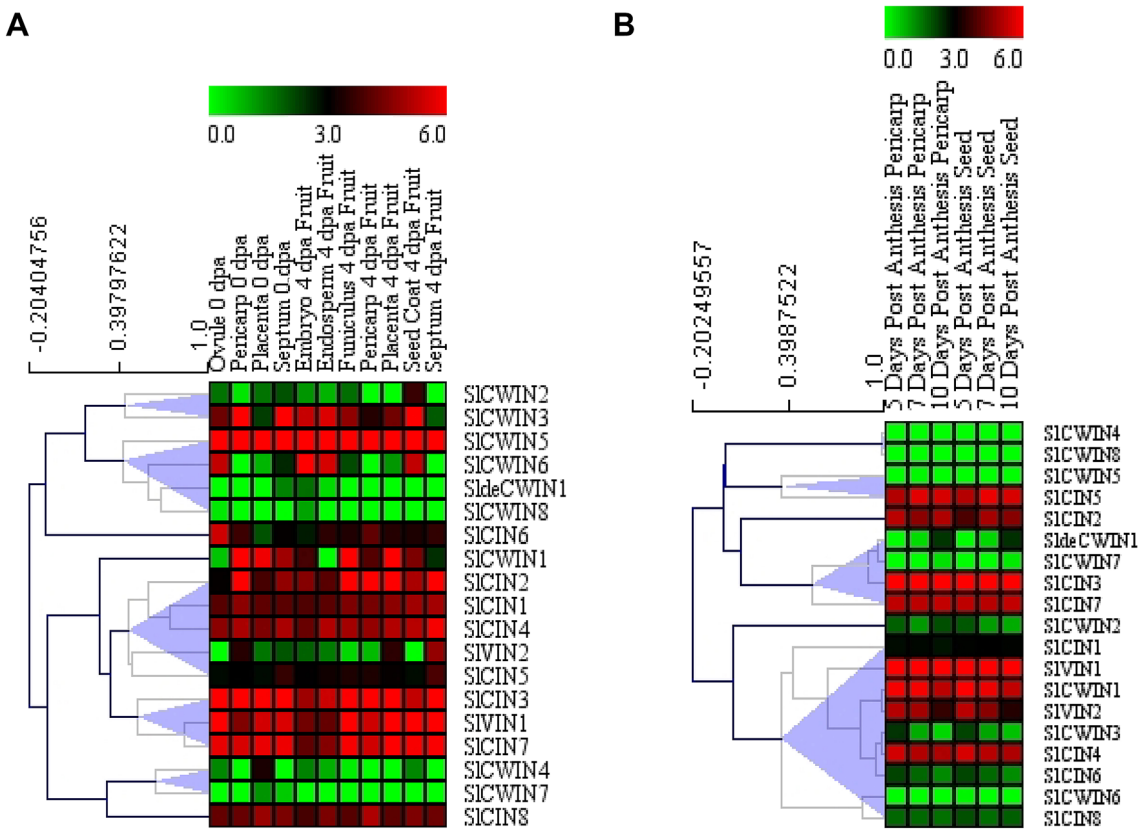

Fig. 5 Expression patterns of invertase genes in tomato. **a** and **b** Expression profiles of 19 detected invertase genes in different tissues from the wild tomato (*S. pimpinellifolium*, LA1589) and cultivated tomato. The two sets of RNA-Seq data (D004 and D005) used for the construction of the heat maps were available in https://ted.bti.cornell.edu/. Clustering was performed with MeV4.5. Red, black and green indicate strong, weak and no expression, respectively

Paralogs from a given invertase subfamily exhibits different responses to abiotic stress

It was well known that abiotic stresses seriously affect plant growth and development, including low or high temperature (Zhao et al. 2018; Zhou et al. 2018; Zhang et al. 2018; Lin et al. 2010), excessive water (Sun et al. 2018), and heavy metals (Lu et al. 2017; Li et al. 2018). In this study, we further examined the expression responses of selected invertase genes to abiotic stress treatments, including NaCl, PEG, cold and heat in *S. lycopersicum* seedlings. The analyses revealed that different members within each invertase subgroup responded differently to the same set of abiotic stresses. For example, among the four *CWIN* genes, *SlCWIN1* (*LIN5*) and *SlCWIN3* (*LIN7*) were repressed at 1.5 h after all the stress treatments whereas their paralog, *SlCWIN 2* did not show this response (Fig. 6). In the *VIN* gene subfamily, *SlVIN2* was dramatically repressed by the all the abiotic stresses, while *SlVIN1* was evidently induced by all the stresses (Fig. 6). Similarly, within the CIN group, *SlCIN1* and *5* were repressed within 1.5 h after stress treatments. On the other hand, the expressions of *SlCIN3*, *4*, and *6* to *8* were enhanced or induced by the stress treatments (Fig. 6). Interestingly, for those repressed, they were able to able to more or less recover their transcript level at 24 h after treatments (Fig. 6).

Discussion

The tomato genome encodes a large number of pseudo or defective invertase genes

Of the 13 putative acid invertase sequences identified, two are pseudogenes owing to the lack of significant portions of coding regions or the presence of stop codons in the coding sequences (Supplemental Table S2). Moreover, among the 9 putative CWINs, five were found to lack the critical β-fructosidase motif or other amino acids required for the enzyme to hydrolyze sucrose, rendering them defective or non-functional CWINs. The presence of such a high proportion of pseudogenes and non-functional paralogs (10/24 = 42%) may indicate their potential role in the evolution of invertase genes. Alternatively, the biochemically

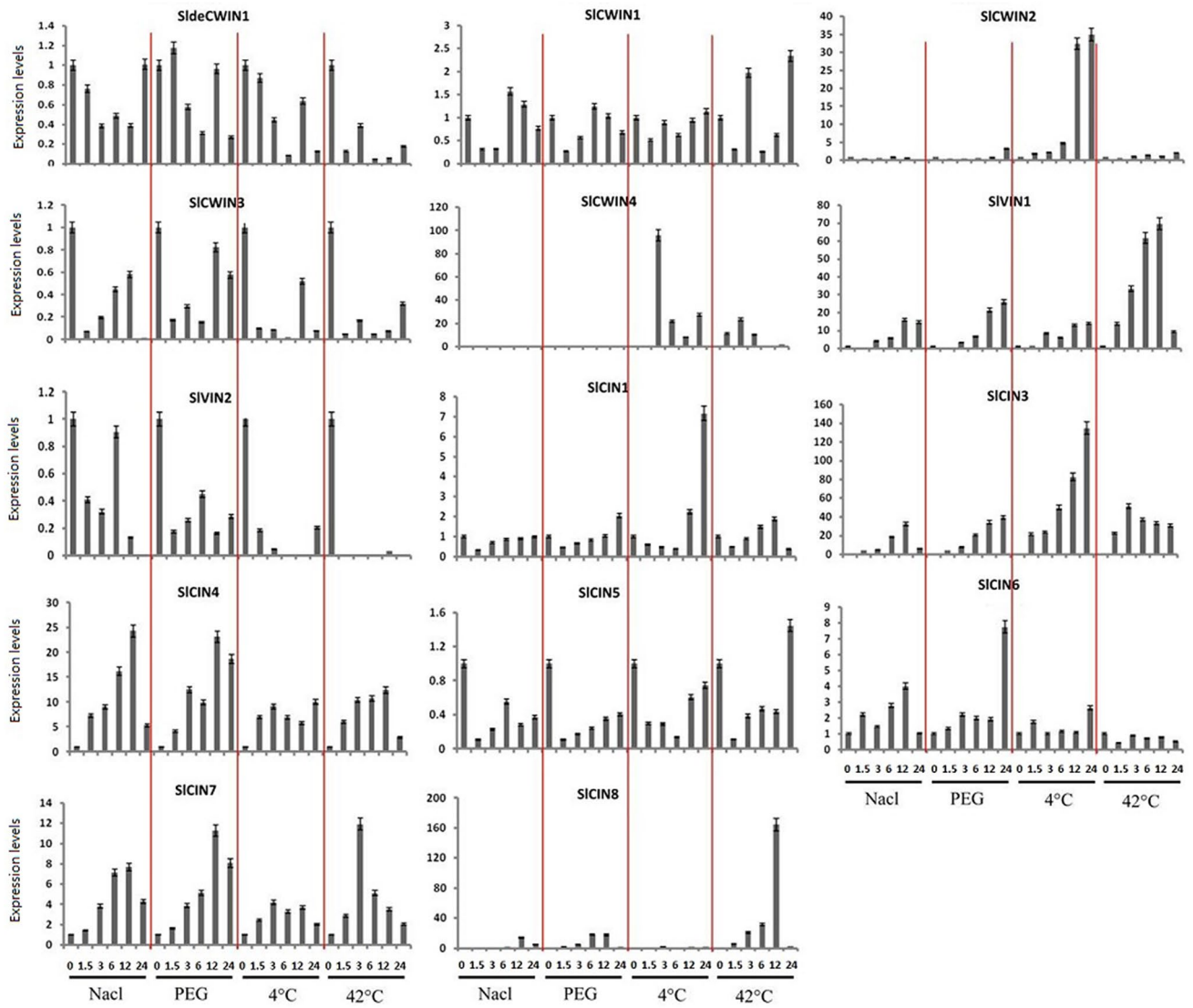

Fig. 6 Transcript levels of invertase members were measured from leaves collected from seedlings at 4th true leaf stage at 0, 1.5, 3, 6, 12 and 24 h after treatment. Each value is the mean ± standard deviations of three biological replicates

defective CWINs may have unknown physiological roles. For example, a defective CWIN in tobacco, *Nin88*, has been shown to modulate CWIN activity in vitro (Sturm and Chrispeels 1990). It remains to be determined if any of the 4 tomato defective CWINs plays roles in regulating invertase activity.

Genetic vatations of CWIN invertases in cultivatied tomato and wild tomato (*S. pennellii*)

This study also revealed high conservation in structural features of invertase genes between the cultivated *S. lycopersicum* and the wild species *S. pimpinellifolium*. This is indicated by, for example, the similar number of CWIN gene sequences in the two species, being 9 in the former and 9 in the latter including 5 non-functional invertsase sequences in each (Supplemental Table S2). By contrast, 11 CWIN invertase genes were found in the genome of *S. pennellii* (Supplemental Table S2), another wild tomato species (Bolger et al. 2014). Therefore, genetic vatations of CWIN invertases were occurred during the course of evolution in tomato.

Differential stress responses from paralogs within a given subfamily indicate functional plasticity and evolution adaptability of invertases

During evolution, plants must develop a capacity to cope with environmental stresses at the gene expression level (Xu et al. 2014; Ma et al. 2012; Liu et al. 2013; Wang et al.

2011). To this end, it is evident that paralogs within each invertase subgroup responded differently to salt, PEG and high or low temperature treatments (Fig. 6). Typically, some members were repressed by the stress whereas others were induced or enhanced by the same treatments, a phenomenon observed across all the CWIN, VIN and CIN subfamilies (Fig. 6). The finding is reminiscent to the opposite response of paralogs to sugar availability for VIN and Sus gene families in maize (Xu et al. 1996). Our results, together with those reported by Xu et al (1996), indicate that such a contrasting response may be a common feature across all the invertase gene families in eudicot species of tomato and the monocot maize. Recently, it has been shown that gene expression diversity plays a positive role in the adaptation of *Miscanthus lutarioriparius* to water limitation (Xu et al. 2015).

In conclusion, our genomic and phylogenetic analyses performed on tomato and other species revealed contrasting evolutionary patterns between acid and neutral/alkaline invertases. The CINs had been subjected to stronger purifying selection than the CWIINs and VINs during their evolution in tomato and potato. This, together with the high number of CINs as compared to that of CWINs and VINs in a given species (Ruan 2014), may reflect the need to maintain stable and robust CIN activity, hence cytosolic sugar hemostasis during evolution, which is vital for cellular function. We also identified a larger number of pseudo/non-functional/defective CWINs in tomato and other species. They may play roles in the evolution of new genes through recombination and gene conversion (Brosius and Gould 1992; Michelmore and Meyers 1998). Alternatively, some of the defective CWINs may have physiological roles in modulating CWIN activity (Sturm and Chrispeels 1990). Finally, paralogs within each of the CWIN, VIN and CIN subfamilies exhibited diverse responses to a range of abiotic stress treatments, probably reflecting functional adaptability of the invertase genes during plant evolution.

Acknowledgements The authors would like to thank Prof. Yong-Ling Ruan for conceptualizing preliminarily the experiments.

Author contributions H.W. and S.C. conceived and designed the research. L.R., L.P., Y.C, M.R., Q.Y., performed the experiments. Z.Y., G.Z., R.W., Y.C. and H.W. analyzed the data and wrote the paper. H.W. revised the manuscript. All authors read and approved the final manuscript.

Funding This research was partially supported by National Key Research and Development Program of China (2017YFD0101902), State Key Laboratory Breeding Base for the Zhejiang Sustainable Pest and Disease Control (2010DS700124-ZZ1903 and 2010DS700124-ZZ1807), National Natural Science Foundation of China (31772294), National Key Research and Development Program (2018YCGC005), Zhejiang Provincial Major Agricultural Science and Technology Projects of New Varieties Breeding (2016C02051), Zhejiang Provincial Natural Science Foundation of China (LY18C150008), General Program from the National key research and development program (2018YFD1000800), The earmarked fund for China Agriculture Research System (CARS-23-G-44).

Compliance with ethical standards

Conflicts of interest The authors declare no conflicts of interest.

References

Abascal F, Zardoya R, Posada D (2005) ProtTest: selection of best-fit models of protein evolution. Bioinformatics 21:2104–2105

Alberto F, Bignon C, Sulzenbacher G, Henrissat B, Czjzek M (2004) The three-dimensional structure of invertase (beta-fructosidase) from *Thermotoga maritima* reveals a bimodular arrangement and an evolutionary relationship between retaining and inverting glycosidases. J Med Chem 279:18903–18910

Barratt DHP, Derbyshire P, Findlay K, Pike M, Wellner N, Lunn J, Feil R, Simpson C, Maule AJ, Smith M (2009) Normal growth of *Arabidopsis* requires cytosolic invertase but not sucrose synthase. Proc Natl Acad Sci USA 106:13124–13129

Beauvoit BP, Colombié S, Monier A, Andrieu MH, Biais B, Bénard C, Chéniclet C, Dieuaide-Noubhani M, Nazaret C, Mazat JP, Gibon Y (2014) Model-assisted analysis of sugar metabolism throughout tomato fruit development reveals enzyme and carrier properties in relation to vacuole expansion. Plant cell 26:3224–3242

Bolger A, Scossa F, Bolger ME, Lanz C, Maumus F, Tohge T, Quesneville H, Alseekh S, Sørensen I, Fich EA, Conte M, Keller H, Schneeberger K, Schwacke R, Ofner I, Vrebalov J, Xu Y, Osorio S, Aflitos SA, Schijlen E, Jiménez-Goméz JM, Ryngajllo M, Kimura S, Kumar R, Koenig D, Headland LR, Maloof JN, Sinha N, van Ham RC, Lankhorst RK, Mao L, Vogel A, Arsova B, Panstruga R, Fei Z, Rose JK, Zamir D, Carrari F, Giovannoni JJ, Weigel D, Usadel B, Fernie AR (2014) The genome of the stress-tolerant wild tomato species *Solanum pennellii*. Nat Genet 46:1034–1038

Braun DM, Wang L, Ruan YL (2014) Understanding and manipulating sucrose phloem loading unloading metabolism and signalling to enhance crop yield and food security. J Exp Bot 65:1713–1735

Brosius J, Gould S (1992) On "genomenclature": a comprehensive (and respectful) taxonomy for pseudogenes and other "junk DNA". Proc Natl Acad Sci USA 89:10706–10710

Cannon SB, Mitra A, Baumgarten A, Young ND, May G (2004) The roles of segmental and tandem gene duplication in the evolution of large gene families in *Arabidopsis thaliana*. BMC Plant Biol 4:10

Chen MY, Li K, Li HP, Song CP, Miao YC (2017) The glutathione peroxidase gene family in *Gossypium hirsutum*: Genome-wide identification classification gene expression and functional analysis. Sci Rep 7:44743

Cheng WH, Tallercio EW, Chourey PS (1996) The Miniature1 seed locus of maize encodes a cell wall invertase required for normal development of endosperm and maternal cells in the pedicel. Plant Cell 8:971–983

Expósito-Rodríguez M, Borges AA, Borges-Pérez A, Pérez JA (2008) Selection of internal control genes for quantitative real-time RT-PCR studies during tomato development process. BMC Plant Biol 8:131

Fridman E, Carrari F, Liu YS, Fernie AR, Zamir D (2004) Zooming in on a quantitative trait for tomato yield using interspecific introgressions. Science 305:1786–1789

Fridman E, Zamir D (2003) Functional divergence of a syntenic invertase gene family in tomato potato and *Arabidopsis*. Plant Physiol 131:603–609

Guo SY, Dai SJ, Singh PK, Wang HY, Wang YN, Tan JLH, Wee WY, Ito T (2018) A membrane-bound NAC-like transcription factor OsNTL5 represses the flowering in *Oryza sativa*. Front Plant Sci 9:555

Gao W, Xu FC, Guo DD, Zhao JR, Liu J, Guo YW, Singh PK, Ma XN, Long L, Botella JR, Song CP (2018) Calcium-dependent protein kinases in cotton: insights into early plant responses to salt stress. BMC Plant Biol 18(1):15

Godt DE, Roitsch T (1997) Regulation and tissue-specific distribution of mRNAs for three extracellular invertase isoenzymes of tomato suggests an important function in establishing and maintaining sink metabolism. Plant Physiol 115:273–282

Gu X (2006) A simple statistical method for estimating type-II (cluster-specific) functional divergence of protein sequences. Mol Biol Evol 23:1937–1945

Gu X (1999) Statistical methods for testing functional divergence after gene duplication. Mol Biol Evol 16:1664–1674

Gu X, Zou Y, Su Z, Huang W, Zhou Z, Arendsee Z, Zeng X (2013) An update of DIVERGE software for functional divergence analysis of protein family. Mol Biol Evol 30(7):1713–1719

Guindon S, Gascuel O (2003) A simple, fast, and accurate algorithm to estimate large phylogenies by maximum likelihood. Syst Biol 52:696–704

Guo YW, Guo HL, Li X, Huang LL, Zhang BN, Pang XB, Liu BY, Ma LQ, Wang H (2013) Two type III polyketide synthases from *Polygonum cuspidatum*: gene structure evolutionary route and metabolites. Plant Biotechnol Rep 7(3):371–381

Jin Y, Ni DA, Ruan YL (2009) Posttranslational elevation of cell wall invertase activity by silencing its inhibitor in tomato delays leaf senescence and increases seed weight and fruit hexose level. Plant Cell 21:2072–2089

Ji X, Wim EVD, Laere AV, Cheng SH, Bennett J (2005) Structure evolution and expression of the two invertase gene families of rice. J Mol Evol 60:615–634

Lammens W, Le RK, Schroeven L, Van Laere A, Rabijns A, Van den Ende W (2009) Structural insights into glycoside hydrolase family 32 and 68 enzymes: functional implications. J Exp Bot 60:727–740

Le Roy K, Vergauwen R, Struyf T, Yuan S, Lammens W, Mátrai J, De Maeyer M, Van den End W (2013) Understanding the role of defective invertases in plants: tobacco Nin88 fails to degrade sucrose. Plant Physiol 161(4):1670–1681

Li L, Hou MJ, Cao L, Xia Y, Shen ZG, Hu ZB (2018) Glutathione S-transferases modulate Cu tolerance in *Oryza sativa*. Environ Exp Bot 155:313–320

Li ZM, Palmer WM, Martin AP, Wang RQ, Rainsford F, Jin Y, Patrick JW, Yang YJ, Ruan YL (2012) High invertase activity in tomato reproductive organs correlates with enhanced sucrose import into, and heat tolerance of, yound fruit. J Exp Bot 63(3):1155–1166

Liu LY, Li LN, Yao CP, Meng SS, Song CP (2013) Functional analysis of the ABA-responsive protein family in ABA and stress signal transduction in *Arabidopsis*. Chin Sci Bull 58(31):3721–3730

Liu YH, Offler CE, Ruan YL (2016) Cell wall invertase promotes fruit set under heat stress by suppressing ROS-independent cell death. Plant Physiol 172(1):163–180

Livak KJ, Schmittgen TD (2001) Analysis of relative gene expression data using real time quantitative PCR and $2^{-\Delta\Delta Ct}$ method. Methods 25(4):402–408

Lin DL, Xia JY, Wan SQ (2010) Climate warming and biomass accumulation of terrestrial plants: a meta-analysis. New Phytol 188:187–198

Lou Y, Gou JY, Xue HW (2007) PIP5K9, an Arabidopsis phosphatidylinositol monophosphate kinase interacts with a cytosolic invertase to negatively regulate sugar mediated root growth. Plant Cell 19:163–181

Lu T, Zhang G, Sun L, Wang J, Hao F (2017) Genome-wide identification of CBL family and expression analysis of CBLs in response to potassium deficiency in cotton. Peer J 5:e3653

Lü D, Wang W, Miao C (2013) ATHK1 acts downstream of hydrogen peroxide to mediate ABA signaling through regulation of calcium channel activity in Arabidopsis guard cells. Chin Sci Bull 58(3):336–343

Ma LY, Zhang H, Sun LR, Jiao YH, Zhang GZ, Miao C, Hao FS (2012) NADPH oxidase AtrbohD and AtrbohF function in ROS-dependent regulation of Na^+/K^+ homeostasis in Arabidopsis under salt stress. J Exp Bot 63(1):305–317

Mathias NA, Folkard A, Yong W, Christian RJ, Henrik N, Vagn OM, Karen K (2002) Soluble invertase expression is an early target of drought stress during the critical, abortion-sensitive phase of young ovary development in maize. Plant Physiol 130(2):591–604

Michelmore RW, Meyers BC (1998) Clusters of resistance genes in plants evolve by divergent selection and a birth-and-death process. Genome Res 8:1113–1130

Murayama S, Handa H (2007) Genes for alkaline/neutral invertase in rice: alkaline/neutral invertases are located in plant mitochondria and also in plastids. Planta 225:1193–1203

Nelson BK, Cai X, Nebenführ A (2007) A multicolored set of in vivo organelle markers for co-localization studies in Arabidopsis and other plants. Plant J 51:1126–1136

Paiva EAS, Sampaio RA, Martinez HEP (1998) Composition and quality of tomato fruit cultivated in nutrient solutions containing different calcium concentrations. J Plant Nutr 21(12):2653–2661

Pan LZ, Guo QW, Chai SL, Cheng Y, Ruan MY, Ye QJ, Wang RQ, Yao ZP, Zhou GZ, Li ZM, Deng MH, Jin FM, Liu LC, Wan HJ (2019) Evolutionary conservation and expression patterns of neutral/alkaline invertases in *Solanum*. Biomolecules 9:763

Pang YQ, Li JT, Qi BS, Tian M, Sun LR, Wang XC, Hao FS (2017) Aquaporin AtTIP5,1 as an essential target of gibberellins promotes hypocotyl cell elongation in *Arabidopsis thaliana* under excess boron stress. Func Plant Biol 45(3):305–314

Qian WJ, Xiao B, Wang L, Hao XY, Yue C, Cao HL, Wang YC, Li NN, Yu YB, Zeng JM, Yang YJ, Wang XC (2018) *CsINV5*, a tea vacuolar invertase gene enhances cold tolerance in transgenic Arabidopsis. BMC Plant Biol 18:228

Ronquist F, Huelsenbeck JP (2003) MrBayes 3: Bayesian phylogenetic inference under mixed models. Bioinformatics 19:1572–1574

Ruan YL (2014) Sucrose metabolism: gateway to diverse carbon use and sugar signaling. Annu Rev Plant Biol 65:33–67

Ruan YL, Jin Y, Yang YJ, Li GJ, Boyer JS (2010) Sugar input metabolism and signaling mediated by invertase: roles in development yield potential and response to drought and heat. Mol Plant 3:942–955

Saeed AI, Sharo V, White J, Li J, Liang W, Bhagabati N, Braisted J, Klapa M (2003) TM4: a free open source system for microarray data management and analysis. Bio Techniques 34:374–378

Schroeven L, Lammens W, Van LA, Van den Ende W (2008) Transforming wheat vacuolar invertase into a high affinity sucrose: sucrose 1-fructosyltransferase. New Phytol 180:822–831

Sturm A, Chrispeels MJ (1990) cDNA cloning of carrot extracellular beta-fructosidase and its expression in response to wounding and bacterial-infection. Plant Cell 2:1107–1119

Sun LR, Ma LY, He SB, Hao FS (2018) AtrbohD functions downstream of ROP2 and positively regulates waterlogging response in Arabidopsis. Plant Signal Behav 13(9):1–5

Sun Q, Wang GH, Zhang X, Zhang XR, Qiao P, Long L, Yuan YL, Cai YF (2017) Genome-wide identification of the TIFY gene family in three cultivated *Gossypium* species and the expression of JAZ genes. Sci Rep 7:42418

Tamura K, Peterson D, Peterson N, Stecher G, Nei M, Kumar S (2011) MEGA5: molecular evolutionary genetics analysis using

maximum likelihood evolutionary distance and maximum parsimony methods. Mol Biol Evol 28:2731–2739

Thompson JD, Gibson TJ, Plewniak F, Jeanmougin F, Higgins DG (1997) The CLUSTAL_X windows interface: flexible strategies for multiple sequence alignment aided by quality analysis tools. Nucleic Acids Res 25:4876–4882

Wang E, Wang J, Zhu X, Hao W, Wang L, Li Q, Zhang L, He W, Lu B, Lin H, Ma H, Zhang G, He Z (2008) Control of rice grain-filling and yield by a gene with a potential signature of domestication. Nat Genet 40:1370–1374

Wang L, Cook A, Patrick JW, Chen XY, Ruan YL (2014) Silencing vacuolar invertase gene GhVIN1 blocks cotton fiber initiation from ovule epidermis probably by suppressing a cohort of regulatory genes via sugar signaling. Plant J 78:686–696

Wang L, Li XR, Lian H, Ni DA, He YK, Chen XY, Ruan YL (2010) Evidence that high activity of vacuolar invertase is required for cotton fiber and Arabidopsis root elongation through osmotic dependent and independent pathways respectively. Plant Physiol 154:744–756

Wang TP, Liu H, Hua HJ, Wang L, Song CP (2011) A vacuole localized beta-glucosidase contributes to drought tolerance in *Arabidopsis*. Chin Sci Bull 56:3538–3546

Welham T, Pike J, Horst I, Flemetakis E, Katinakis P, Kaneko T, Sato S, Tabata S, Perry J, Parniske M, Wang TL (2009) A cytosolic invertase is required for normal growth and cell development in the model legume *Lotus japonicas*. J Exp Bot 60(12):3353–3365

Xiang L, Le RK, Bolouri-Moghaddam MR, Vanhaecke M, Lammens W, Rolland F, Van den Ende W (2011) Exploring the neutral invertase–oxidative stress defence connection in *Arabidopsis thaliana*. J Exp Bot 62:3849–3862

Xu J, Avigne WT, McCarty DR, Koch KE (1996) A similar dichotomy of sugar modulation and developmental expression affects both paths of sucrose metabolism: evidence from a maize invertase gene family. Plant Cell 8:1209–1220

Xu LH, Wang WY, Guo JJ, Qin J, Shi DQ, Li YL, Xu J (2014) Zinc improves salt tolerance by increasing reactive oxygen species scavenging and reducing Na^+ accumulation in wheat seedlings. Biol Plant 58(4):751–757

Xu Q, Xing S, Zhu C, Wei LW, Fan Y, Wang Q, Song Z, Wenhui YW, Luo F, Shan F, Kang L, Chen W, Yan J, Li J, Sang T (2015) Population transcriptomics reveals a potentially positive role of expression diversity in adaptation. J Integr Plant Biol 57:284–299

Yang SH, Gu TT, Pan CY, Feng ZM, Ding J, Hang YY, Chen JQ, Tian DC (2008) Genetic variation of NBS-LRR class resistance genes in rice lines. Theor Appl Genet 116(2):165–177

Zhang G, Lu T, Miao W, Sun L, Tian M, Wang J, Hao F (2017) Genome-wide identification of ABA receptor PYL family and expression analysis of PYLs in response to ABA and osmotic stress in *Gossypium*. Peer J 5:e4126

Zhang H, Yue MX, Zheng XK, Gautam M, He SB, Li LJ (2018) The role of promoter-associated histone acetylation of haem oxygenase-1 (HO-1) and giberellic acid-stimulated like-1 (GSL-1) genes in heat-induced lateral root primordium inhibition in maize. Front Plant Sci 9:1520

Zhao Q, Chen WX, Bian JY, Xie H, Li Y, Xu CX, Ma J, Guo SY, Chen JY, Cai XF, Wang LX, Wang QH, She YM, Chen SX, Zhou ZQ, Dai SJ (2018) Proteomics and phosphoproteomics of heat stress-responsive mechanisms in spinach. Front Plant Sci 9:800

Zhao X, Wang YL, Qiao XR, Wang J, Wang LD, Xu CS, Zhang X (2013) Phototropins function in high-intensity blue light-induced hypocotyl phototropism in Arabidopsis by altering cytosolic calcium. Plant Physiol 162(3):1539–1551

Zhou HR, Xu M, Hou RX, Zheng YP, Chi YG, Ouyang Z (2018) Thermal acclimation of photosynthesis to experimental warming is season dependent for winter wheat (*Triticum aestivum* L.). Environ Exper Bot 150:249–259